



Assessment of stability differences among various grassland biomes under severe drought in the northern China and Tibetan Plateau

Haile Zhao^a, Yi Zhou^b, Xin Chen^c, Yuan Qi^d, Yuyang Chang^e, Yuchao Luo^a, Xingjie Yin^a, Yuling Jin^a, Zhihua Pan^f, Pingli An^{a,*}

^a College of Land Science and Technology, China Agricultural University, Beijing 100193, China

^b School of Geographical Sciences, Hunan Normal University, Changsha 410081, China

^c Institute of Loess Plateau, Shanxi University, Taiyuan 030006, China

^d College of Economics and Management, Northwest A&F University, Yangling 712100, China

^e Department of Environmental Systems Science, ETH Zürich, Zürich 8092, Switzerland

^f College of Resources and Environmental Science, China Agricultural University, Beijing 100193, China



ARTICLE INFO

Keywords:

Ecosystem stability
Grassland
Drought
CMIP6

ABSTRACT

Understanding grassland stability under severe drought is essential for promoting sustainable management in Northern China and Tibetan Plateau (NCTP). However, the differences in stability among various grassland biomes in response to severe drought remain unknown in the NCTP. Therefore, we quantified the temporal stability, drought resistance, and drought resilience of various grassland biomes in the NCTP. Our findings indicated that alpine grasslands exhibited higher stability compared to temperate grasslands, due to their greater drought resistance. This was attributed to the higher biodiversity, precipitation and radiation, and lower temperatures in alpine grasslands, which reduce drought exposure and sensitivity. Drought resilience was similar across grassland biomes, particularly in temperate regions. CMIP6-based projections indicated that future changes in the stability of grasslands in the NCTP exhibited an increasing trend. These findings offer a scientific reference for assessing the impacts of climate change on vegetation growth and carbon cycling in the NCTP.

1. Introduction

Grasslands constitute a crucial component of the global terrestrial ecosystem and represent one of the most prevalent vegetation types, covering roughly 25 % of the Earth's terrestrial surface (Liu et al., 2019b). Recent research indicates that semi-arid grassland ecosystems play a dominant role in driving temporal changes in global vegetation productivity and terrestrial carbon sequestration (Ahlström et al., 2015; Poultre et al., 2014). In China, nearly 30 % of the land area is covered by grasslands, with 87 % situated in Northern China and the Tibetan Plateau (NCTP) (Yang and Huang, 2021). These grasslands offer vital ecosystem services, including livestock production, climate regulation, carbon sequestration, soil erosion control, and biodiversity conservation (Bai et al., 2018; Guo et al., 2021; Hossain et al., 2022). The NCTP is an arid and semi-arid region characterized by ecological fragility, stemming from scarce water resources, sparse vegetation cover, and soil

vulnerability to wind and water erosion (Zhang et al., 2023a). Grasslands, being the predominant vegetation type in the NCTP, provide fundamental support for the local ecological environment. Moreover, their ecosystem stability is pivotal in mitigating ecological degradation in China's arid and semi-arid regions (Zhao et al., 2020). However, climate change, manifested through rising temperatures, along with anthropogenic activities such as overgrazing, is exerting immense pressure on the growth and resilience of grasslands (Liu et al., 2019a; Zhu et al., 2023). Therefore, it is imperative to conduct further research on the stability of grassland productivity and the underlying mechanisms driving its changes in the NCTP.

Over the past two decades, vegetation greening in the NCTP has markedly increased, driven by CO₂ fertilization effects (Piao et al., 2020), large-scale ecological restoration projects (Dou et al., 2024), and enhanced by increased precipitation (Zhang et al., 2023a). However, in the context of global warming, recent decades have witnessed a

* Corresponding author.

E-mail addresses: b20213211003@cau.edu.cn (H. Zhao), zhou_yi@hunnu.edu.cn (Y. Zhou), chenxin@sxu.edu.cn (X. Chen), quan@nwafu.edu.cn (Y. Qi), yuyang_chang@usys.ethz.ch (Y. Chang), row@cau.edu.cn (Y. Luo), ystar.jony@gmail.com (X. Yin), 18758031319@163.com (Y. Jin), panzihua@cau.edu.cn (Z. Pan), anpl@cau.edu.cn (P. An).

dramatic increase in the frequency and intensity of drought events (AghaKouchak et al., 2020). Drought events can profoundly impact the stability of terrestrial ecosystem structure and function, by reducing plant photosynthetic capacity (Piao et al., 2019), decreasing ecosystem net primary productivity (Zhao and Running, 2010), and exacerbating the decline of terrestrial carbon sinks (Sippel et al., 2018). Thus, although the greening of grasslands in the NCTP is primarily bolstered by increased precipitation (Zhao et al., 2020), drought events in the region are anticipated to become more frequent and severe under global warming (Miao et al., 2020), potentially causing even more pronounced disruptions to ecosystem stability (Deng et al., 2021). Given that the NCTP is a water-scarce region, drought serves as the principal factor influencing inter-annual variations in grassland productivity (Li et al., 2020; Zhang et al., 2023a; Zscheischler et al., 2014). Therefore, gaining a deeper understanding of the effects of drought on grassland stability in the NCTP can enhance predictions of ecosystem feedback to future climate change in the region (Friedlingstein et al., 2014), and thus identify ecologically vulnerable areas under future climate change.

As a critical indicator of ecosystem health, stability encompasses both the state of the ecosystem at specific spatial and temporal scales and the sustained ability of the ecosystem to provide services to humans (Montoya et al., 2019; Wang et al., 2019). Currently, the classification of vegetation types in studies of ecosystem stability is broad, predominantly focusing on forest ecosystems (Forzieri et al., 2022; Smith et al., 2020; Zhou et al., 2014). For example, recent research has demonstrated that evergreen broadleaf forests exhibit the highest ecosystem stability, maintaining robust drought resistance despite the increasing impact of drought in recent decades (Huang and Xia, 2019). However, few studies have concentrated on the stability of grassland ecosystems on a regional scale, with numerous types of grassland biomes often grouped into a single category (De Keersmaecker et al., 2015; Ivits et al., 2016; Liu et al., 2023b; Yao et al., 2024), thereby obscuring differences in ecosystem stability among various grassland biomes. Under varying climatic conditions, the species composition, biodiversity, and available water of grassland ecosystems differ (Chen et al., 2021b; Guo et al., 2021; Liu et al., 2019a), leading to variations in their ability to cope with external disturbances. The variability of ecosystem stability among different grassland biomes remains unclear in the NCTP.

To advance the research on grassland stability, this paper seeks to

elucidate the heterogeneity of ecosystem stability across various grassland biomes and their natural drivers in the NCTP. Utilizing long-term (1901–2022) SPEI (Standardized Precipitation-Evapotranspiration Index) data, we first identified regions experiencing severe droughts annually and analyzed the drought exposure among various grassland biomes. Subsequently, employing annual drought and NDVI (Normalized Difference Vegetation Index) data, we assessed the temporal stability of NDVI, along with the resistance and resilience of NDVI to drought among various grassland biomes. We further applied machine learning algorithms to evaluate the relative importance and marginal effect of climatic and biological variables on the temporal stability of grassland NDVI. Finally, we projected future changes in grassland stability based on CMIP6.

2. Materials and methods

2.1. Study area and grassland biomes

Grasslands are the dominant land cover type in the NCTP, comprising 46 % of the NCTP area (Fig. 1). The land cover data for this study were derived from the MCD12C1 v6.1 product of MODIS, spanning the period from 2001 to 2022 with a spatial resolution of 0.05°. We used vegetation classification criteria of the International Geosphere-Biosphere Program (IGBP) to identify the non-woody grasslands (dominated by herbaceous plants under 2 m) in the NCTP as the land cover type for this study. To ensure that subsequent analyses were unaffected by land cover changes, we extracted regions within the NCTP where the land cover type remained consistently grassland throughout 2001–2022, using the Google Earth Engine (GEE) platform (<https://earthengine.google.com/>). According to the classification in the digitized 1:1000,000 Vegetation Atlas of China derived from field surveys (Zhang et al., 2007), grasslands in the NCTP were categorized into five types: temperate meadow steppe (TMS), temperate typical steppe (TTS), temperate desert steppe (TDS), alpine meadow steppe (AMS), and alpine typical steppe (ATS) (Fig. S3). Specifically, we overlay grassland cover data and the Vegetation Atlas of China in ArcGIS 10.7 to classify grassland types in the NCTP.

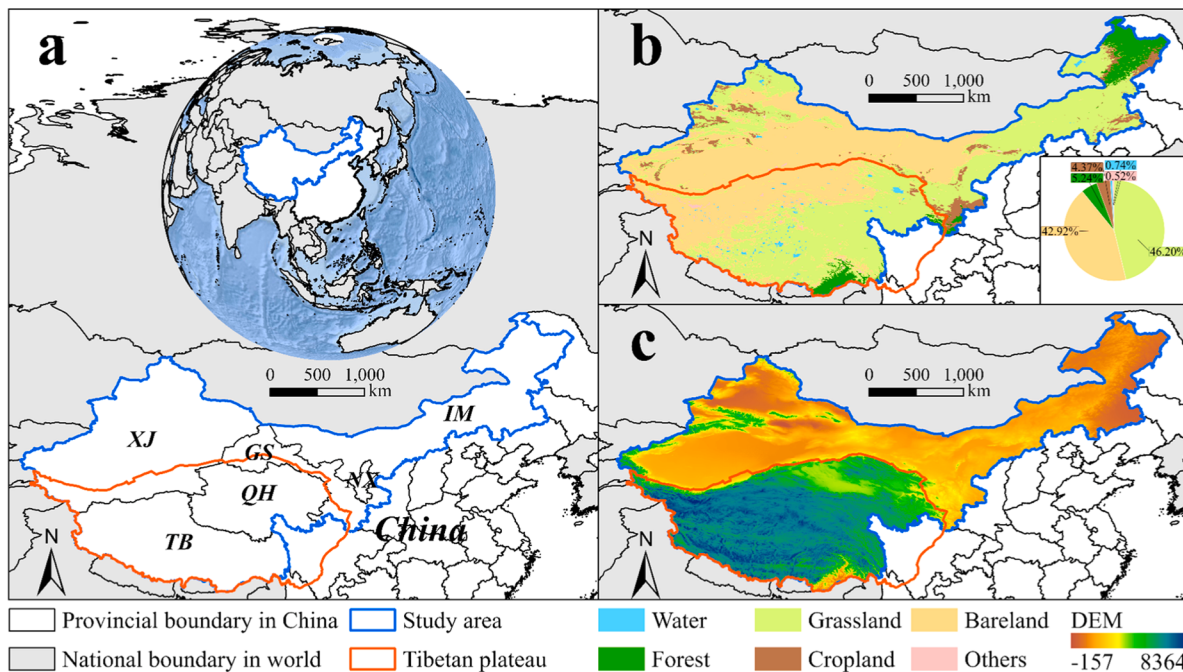


Fig. 1. Overview of the study area. (a) Location of the NCTP in the world. (b) Land cover types for 2022 in the NCTP based on MCD12C1. (c) Elevation of the NCTP.

2.2. Data sources and processing

2.2.1. Vegetation index

In recent decades, satellite remote sensing has emerged as a powerful tool for monitoring vegetation growth dynamics (Forzieri et al., 2022; Li et al., 2020; Yao et al., 2024). Vegetation index data from MODIS have been widely used as the proxy for vegetation greenness, providing an opportunity to characterize the dynamics of photosynthetic productivity in terrestrial vegetation on a broad scale (Zhang et al., 2017). We obtained the 16-day MODIS NDVI product (MOD13C1 v6.1) from the Google Earth Engine (GEE) platform, covering the period from 2000 to 2022 with a spatial resolution of 0.05°. In the NCTP, the vegetation index for the growing season is representative of vegetation growth throughout the year (Piao et al., 2011). In addition, the NDVI of vegetation is very low during the non-growing season and is susceptible to abnormal values due to snow. Consequently, we aggregated the NDVI data from April to October each year into an annual mean at the pixel level and employed the dynamics of the annual NDVI from 2000 to 2022 to characterize drought-induced variations in grassland productivity.

2.2.2. Identifying severe drought years

To identify and quantify severe drought years, we used the SPEIbase v2.9 dataset spanning 1901–2022 (<https://spei.csic.es/database.html>), classifying each year at the pixel level as either an abnormal year (severely dry or severely wet) or a normal year (Liu et al., 2023b; Slette et al., 2019). The SPEIbase v2.9 dataset offers SPEI data at a 0.5° spatial resolution across multiple time scales (1–48 months) (Isbell et al., 2015; Vicente-Serrano et al., 2010). SPEI data represents either a water surplus or deficit for a given month based on water balance (precipitation and potential evapotranspiration) (Ivits et al., 2013). Considering that grassland growth in the NCTP is primarily constrained by moisture gains and losses during the growing season, we aggregated the monthly SPEI data from April to October each year into an annual mean. Based on the United States Drought Monitor, severe drought and wet years were defined as those that historically occurred less frequently than once per decade (<10th and >90th percentiles for SPEI) (Isbell et al., 2015; Zhang et al., 2023b). Using the SPEI data, we established thresholds for abnormal years (severe drought and severe wetness) at each pixel with an occurrence frequency of less than once per decade, thereby deriving the spatial pattern of drought occurrence for each year of the study period (Fig. S4). Specifically, the smallest 10 % and largest 10 % of all SPEI observations from 1901 to 2022 for each pixel were classified as experiencing severe drought or severe wet, respectively (Zhang et al., 2023b). Thus, 20 % (24 years) of the historical SPEI years (122 years) for each pixel were defined as abnormal years, while the remaining years falling between the drought and wetness thresholds were categorized as normal years. To align with the satellite observations, we extracted and analyzed only the SPEI data for abnormal and normal years from 2000 to 2022, resampling it to 0.05° using bilinear interpolation. Drought severity was measured using the SPEI value, while drought duration was determined by counting the number of months with a monthly SPEI less than -1 during the growing season (Schwalm et al., 2017). All SPEI data processing was conducted using R v4.3.3.

2.2.3. Climate forcing and biodiversity datasets

Climate forcing and biodiversity variables were employed to examine their relative importance and marginal effect on the temporal stability of grassland NDVI in the NCTP (Fig. S5). Climate data, including temperature, precipitation, and shortwave radiation, were derived from the ERA5-Land reanalysis dataset of the Copernicus Climate Data Store. We extracted monthly temperature, precipitation, and shortwave radiation data from ERA5-Land at a spatial resolution of 0.1° and aggregated the April to October data into an annual mean. The annual temperature, precipitation, and shortwave radiation data from 2000 to 2022 were subsequently averaged to derive the mean annual temperature (MAT), mean annual precipitation (MAP), and mean

annual shortwave radiation (MAR). Additionally, we utilized native species richness data as an indicator to quantify grassland biodiversity in the NCTP (Moen et al., 2012). Native species richness data were normalized and converted from vectors to a 0.05° grid in ArcGIS 10.7. All climate and biodiversity data were obtained and processed on the GEE platform and resampled to 0.05° using bilinear interpolation to align with the NDVI data.

2.3. Calculation of stability components

High ecosystem stability of vegetation is demonstrated by a great capacity to withstand external disturbances or recover rapidly from them (Pennekamp et al., 2018). The long-term coefficient of variation of the vegetation index serves as a robust indicator of fluctuations in vegetation growth; a smaller coefficient of variation signifies greater stability in vegetation growth (Wang et al., 2019). Therefore, the coefficient of variation of annual NDVI from 2000 to 2022 was utilized in this study to reflect the stability of grassland ecosystems. The stability is calculated as follows:

$$S = \frac{\mu}{\delta}$$

Where S represents the temporal stability of NDVI. μ represents the mean NDVI from 2000 to 2022. δ represents the NDVI standard deviation from 2000 to 2022.

Two components of temporal stability, namely resistance and resilience, were utilized to evaluate the impact of severe drought on the temporal stability of NDVI. The impact of drought on the temporal stability of ecosystems can generally be characterized by resistance and resilience (De Keersmaecker et al., 2015), with these components capturing both the immediate and lagged effects of drought on ecosystems (Pennekamp et al., 2018). Resistance quantifies the direct impact of drought on ecosystem function, expressed as the ability to maintain normal levels during drought (Van Ruijven and Berendse, 2010). Resilience is defined as the rate at which ecosystem function recovers to its normal state following a drought (Ivits et al., 2016). The metrics for resistance and resilience employed in this study are dimensionless, facilitating direct comparisons between grassland biomes with varying productivity levels. The resistance and resilience are calculated as follows:

$$\Omega = \frac{\bar{Y}_n}{|Y_d - \bar{Y}_n|}$$

$$\Delta = \left| \frac{Y_d - \bar{Y}_n}{Y_{d+1} - \bar{Y}_n} \right|$$

Where Ω and Δ represent resistance and resilience, respectively. \bar{Y}_n represents the mean NDVI during normal years (excluding severe drought and severe wet years). Y_d represents the NDVI for the severe drought year. Y_{d+1} represents the NDVI for the year following the severe drought year. The resistance and resilience during 2000–2022 were calculated as annual averages.

2.4. Random Forest modeling and statistical analysis methods

To identify the key factors influencing the temporal stability of grasslands in the NCTP and their driving mechanisms, we selected four previously reported variables affecting ecosystem stability for Random Forest regression analysis (Huang and Xia, 2019; Liu et al., 2023b; Schwalm et al., 2017; Seddon et al., 2016), including one biological variable (BD) and three climatic variables (MAT, MAP, MAR). Random Forest is an ensemble machine learning algorithm that constructs a collection of regression trees and averages their predictions, with each tree trained on a randomly selected subset of the training data (Breiman, 2001). Random Forest is capable of elucidating interactions and

nonlinear relationships between variables while addressing multicollinearity in multiple regression by distributing the importance of variables across all predictors (Liu et al., 2023a). In this study, the Random Forest algorithm employed 100 binary decision trees, with the parameter Mtry (number of randomly chosen variables) set to 1 (1 variable chosen at random from the full set to determine the splitting rule) and the minimum terminal node size set to 5 (nodes with less than 5 observations cannot be split). To visualize the relationship between explanatory variables and stability, independent of other variables, partial dependence plots derived from the Random Forest algorithm were generated. The partial dependence plot illustrates the marginal effect of a variable on the response variable, where the response variable is explained solely within the context of the explanatory variable (Schwalm et al., 2017). Additionally, we computed the relative importance of each variable using the Random Forest algorithm. The relative importance of each variable was assessed by the percentage increase in the mean square error (%IncMSE) between the variable and stability,

and the final importance ranking was determined by the average absolute error reduction across all decision trees (Huang and Xia, 2019; Liu et al., 2023b). We normalized %IncMSE for all variables, with a higher %IncMSE reflecting greater variable importance.

Two-tailed Mann-Kendall (MK) tests and Theil-Sen slope estimation were employed to quantify linear trends and their significance for NDVI, SPEI, and drought exposure (including drought severity, drought duration, and drought area percentage) during 2000–2022. The detailed description of inter-annual variations in NDVI and SPEI across different grassland biomes is shown in [Supplementary Materials](#). In addition, to verify the significance of differences in stability components among various grassland biomes, the Tukey Honest Significant Differences (TukeyHSD) method was applied to test for mean differences. The TukeyHSD method, based on one-way analysis of variance (ANOVA), identified differences as statistically significant at the $p = 0.05$ level. Geographically Weighted Regression (GWR) as a spatial data analysis method is superior to traditional global regression models in accounting

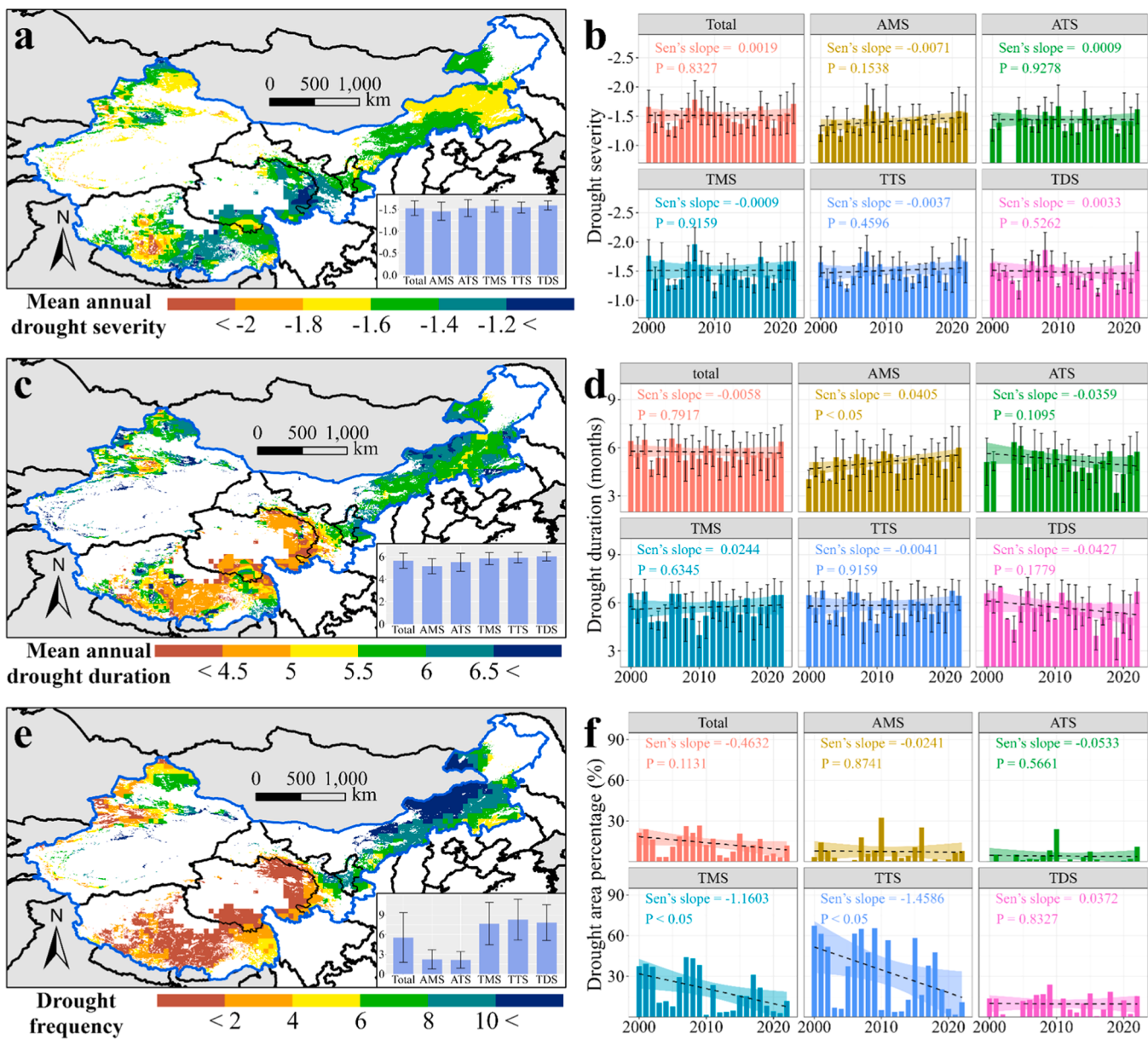


Fig. 2. Drought exposure of grasslands in the NCTP. (a, c, e) Spatial distribution of drought exposure in grasslands. (b, d, f) Temporal change of drought exposure in various grassland biomes (note: error bars indicate one standard error, dashed lines indicate OLS linear regression, and gray areas indicate 95 % confidence intervals).

for spatial data heterogeneity and non-stationarity (Xia et al., 2023; Yang et al., 2024). Random Forest modeling and statistical analyses were conducted in R v4.3.3.

2.5. Predicting changes in grassland ecosystem stability based on CMIP6

To reveal future changes in grassland ecosystem stability, we computed changes relative to the historical period using GPP data from 10 CMIP6 models (Table S1). CMIP6 offers future GPP projections under various combinations of shared socio-economic pathways (SSPs) and representative concentration pathways (RCPs). Specifically, we selected GPP data for the future period (2086–2100) and the historical period (2000–2014) under SSP126, SSP245, and SSP585 scenarios to assess changes in grassland ecosystem stability. SSP126, SSP245, and SSP585 represent low, medium, and high greenhouse gas (GHG) emission pathways for the future (Liu et al., 2023b). Future and historical GPP data for all scenarios were resampled to a 0.05° spatial resolution using bilinear interpolation, and monthly GPP data for the growing seasons were aggregated into annual means.

3. Results

3.1. Drought exposure among different grassland biomes

We conducted an analysis of the exposure of NCTP grasslands to severe drought from 2000 to 2022, revealing significant regional

disparities in drought exposure (Fig. 2a,c,e). Compared to Qinghai and Tibet, grasslands in Inner Mongolia, Xinjiang, Ningxia, and Gansu experienced greater drought severity, longer drought duration, and higher drought frequency. Consequently, drought severity, duration, and frequency were lower in AMS and ATS compared to TMS, TTS, and TDS, indicating that alpine grasslands were less exposed to drought than temperate grasslands throughout the study period. Regarding temporal changes, the drought severity of NCTP grasslands exhibited a non-significant increasing trend, whereas both drought duration and area percentage displayed non-significant decreasing trends (Fig. 2b,d,f). Additionally, the trend in drought exposure varied across different grassland biomes. Specifically, the drought severity of ATS and TDS exhibited non-significant increasing trends, whereas those of AMS, TMS, and TTS displayed non-significant decreasing trends. For drought duration, AMS and TMS respectively exhibited significant ($P < 0.05$) and non-significant increasing trends, while all other grassland biomes displayed non-significant decreasing trends. All grassland biomes exhibited decreasing trends in drought area percentage, with only the trends for TMS and TTS being significant.

3.2. Stability components among different grassland biomes

The temporal stability of NDVI in NCTP grasslands exhibits significant spatial heterogeneity (Fig. 3a). Specifically, the temporal stability of NDVI was lower in the grasslands of Inner Mongolia, Ningxia, and Gansu, while it was higher in the grasslands of Qinghai and Tibet. There

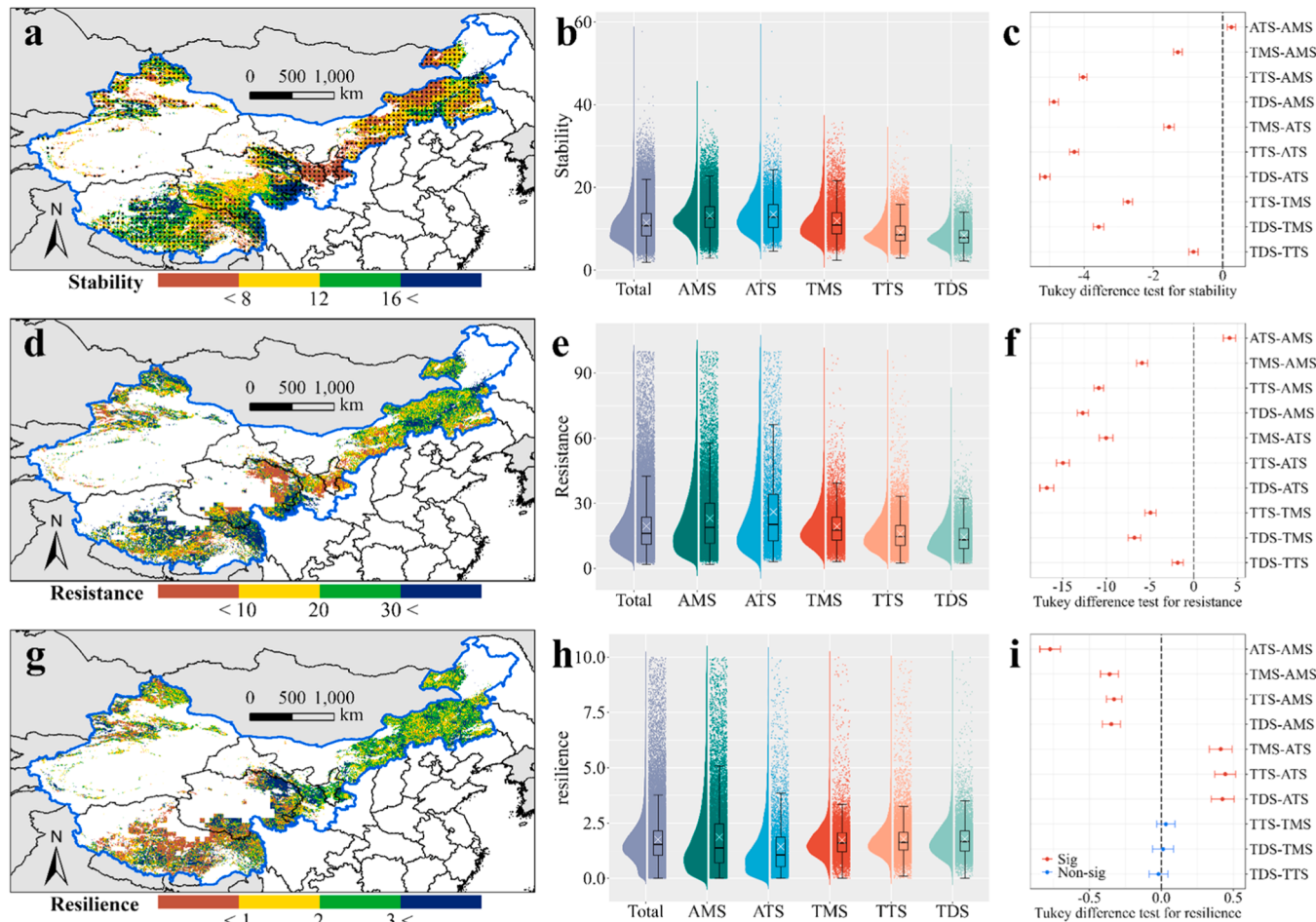


Fig. 3. Temporal stability, drought resistance, and drought resilience of grasslands in the NCTP. (a, d, g) Spatial distribution of stability, resistance, and resilience in grasslands (note: black dots indicate grassland areas with drought identified). (b, e, h) Comparison and (c, f, i) Tukey difference test of stability, resistance, and resilience among different grassland biomes (note: box plots show the middle horizontal line for the median, upper and lower box lines for the 25th and 75th percentiles, white crosses for the mean, and whiskers for 1.5 times the interquartile range).

were also distinct differences in NDVI temporal stability among different grassland biomes (Fig. 3b). AMS and ATS exhibited the highest NDVI temporal stability, followed by TMS and TTS, with TDS showing the lowest stability. This indicates that the NDVI temporal stability of alpine grasslands was significantly higher than that of temperate grasslands. The resistance of NDVI to drought in NCTP grasslands also displayed spatial heterogeneity, with a pattern similar to the temporal stability of NDVI (Fig. 3d). AMS and ATS exhibited significantly higher resistance of NDVI to drought compared to TMS, TTS, and TDS (Fig. 3e). The NDVI recovery rate of grasslands in Qinghai was the highest, followed by those in Inner Mongolia, Xinjiang, Gansu, and Ningxia, with Tibet showing the lowest rate (Fig. 3g). Although the resilience of NDVI to drought exhibited significant differences between alpine and temperate grasslands, the mean difference was minimal, and there was no significant difference in resilience among TMS, TTS, and TDS (Fig. 3h). This suggests that resilience was very similar among grassland biomes. In addition, we calculated the sensitivity of grassland NDVI to drought to validate that alpine grasslands exhibited higher stability compared to temperate grasslands, as described in Supplementary Materials.

3.3. Relative importance and marginal effect of different variables on stability

We examined the relative importance and marginal effect of climatic factors and biodiversity on the temporal stability of NDVI in grasslands across different climate zones. Attribution analysis revealed that MAR and MAT were the primary drivers of grassland stability in the NCTP (Fig. 4). Specifically, variations in MAR and MAT led to substantial spatial differences in grassland stability within the NCTP. MAP and BD were less influential in explaining grassland stability in the NCTP, with relative importance scores below 0.25. However, the principal drivers of changes in grassland stability differed among climate zones (Fig. 4). In alpine regions, MAR and BD were the primary drivers of grassland stability, followed by MAP and MAT. In temperate regions, MAT and MAR were the primary drivers of grassland stability, followed by BD and MAP.

Increases in precipitation, radiation, and biodiversity generally had consistent positive effects on grassland stability, whereas grassland stability exhibited a nonlinear response to temperature changes (Fig. 5). However, there is variability in the marginal effect of these variables on the temporal stability of grasslands across different climate zones (Fig. 5). In alpine regions, grassland stability increases with the rise in various variables. However, when MAP exceeds 700 mm or MAT exceeds 5°C, alpine grassland stability tends to decline. In temperate regions, the response functions of stability are more intricate. In drier ecosystems (MAP < 250 mm), grassland stability tended to decrease with increasing precipitation. However, above this threshold, the

opposite relationship was observed, with grassland stability increasing with higher precipitation levels. This indicates that grassland stability may be higher in areas of severe drought (MAP < 100 mm). Similar to the alpine regions, the stability of temperate grasslands tends to decline when MAT exceeds 10°C. The stability of temperate grasslands increased with rising MAR, but it exhibited a decreasing trend as MAR increased from 3000 to 3200.

3.4. Future changes in grassland stability

Grassland stability derived from model outputs during the historical period was consistent with observational data, both indicating that alpine grasslands exhibit higher stability compared to temperate grasslands (Fig. 3; Fig. S6). We also calculated future changes in the stability of NCTP grassland, demonstrating that grasslands with increasing stability were larger than those with decreasing stability under all three scenarios. (Fig. 6). Under the SSP126 scenario, 67.2 % of grasslands exhibited increasing stability, primarily located in Qinghai, Tibet, and Xinjiang, whereas 32.8 % of grasslands showed decreasing stability, mainly in Inner Mongolia (Fig. 6a-b). Under the SSP245 and SSP585 scenarios, the proportion of grasslands with increasing stability rises to 86.4 % and 98.5 %, respectively (Fig. 6e&h). Furthermore, the increase in the stability of NCTP grassland is anticipated to be greater under the SSP585 scenario compared to the SSP126 and SSP245 scenarios (Fig. 6c, f&i). Notably, the increase in grassland stability is consistently greater in alpine regions compared to temperate regions across all three scenarios. These findings suggest that future concurrent increases in CO₂ concentration, temperature, and precipitation could enhance grassland stability in the NCTP, particularly in the alpine regions.

4. Discussion

4.1. Differences in stability among various grassland biomes

Ecosystem stability is important for the provision of ecosystem services and human well-being (Bengtsson et al., 2019; Guo et al., 2021). Frequent drought events seriously threaten the stability of terrestrial ecosystems (AghaKouchak et al., 2020; Sippel et al., 2018). Especially in grasslands with low precipitation, ecosystems are more vulnerable to drought (Ivits et al., 2016). Many studies have analyzed how grassland stability responds to different types of disturbance (Hautier et al., 2020; Luo et al., 2023; Muraina et al., 2021; Smith et al., 2024). However, fewer studies have been conducted on a regional scale to analyses differences in stability among grasslands in the NCTP. Our study complements related experimental studies in this region. In this study, we found significant differences in stability among different grasslands. Specifically, the stability of alpine grasslands is significantly higher than that

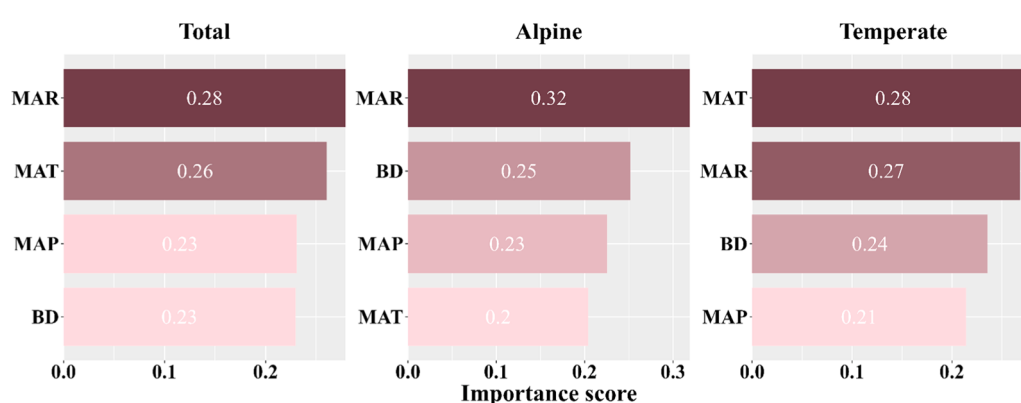


Fig. 4. Relative importance of different variables on stability. The importance score of each variable was assessed by the percentage increase in the mean square error (%IncMSE) between the variable and stability. MAR, MAT, MAP, and BD represent mean annual shortwave radiation, mean annual temperature, mean annual precipitation, and biodiversity, respectively.

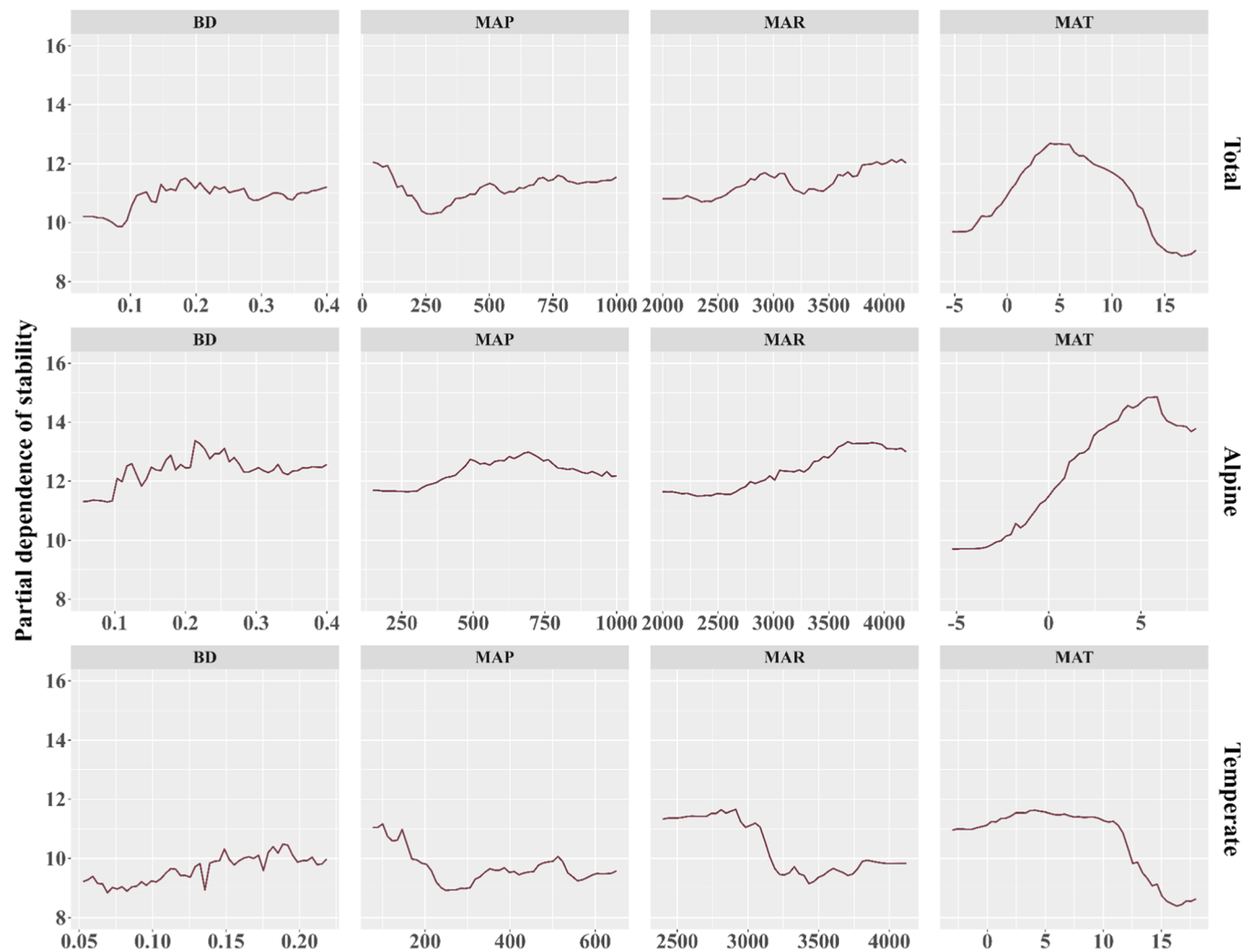


Fig. 5. Marginal effect of different variables on stability. MAR, MAT, MAP, and BD represent mean annual shortwave radiation, mean annual temperature, mean annual precipitation, and biodiversity, respectively.

of temperate grasslands. We then further explored differences in the two components of stability among different grasslands. The results showed that alpine grasslands had significantly higher drought resistance than temperate grasslands, which was consistent with stability. Previous studies have also revealed significant differences in the stability of different ecosystems, with high stability in forest ecosystems also stemming from their high resistance to drought (Huang and Xia, 2019). Drought resistance is primarily related to local climate and biodiversity, and is also influenced by the drought severity and drought duration (Huang et al., 2021; Liu et al., 2023b). We also found that the resilience to drought was similar among grassland biomes in the NCTP, especially among temperate grassland biomes, which was largely due to the similar sensitivity to moisture changes (Seddon et al., 2016) and the common range of water use efficiency (WUE) (Ponce-Campos et al., 2013) among herbaceous biomes. Moreover, grassland productivity recovers rapidly after drought, which explains the very similar resilience to drought among grassland biomes. This is supported by findings that vegetation productivity globally can recover within a year after a drought, indicating no significant differences in resilience across vegetation types at interannual scales (Schwalm et al., 2017).

4.2. Mechanisms of climate and biodiversity effects on grassland stability

Our results suggest that regional climate conditions and biodiversity significantly influence grassland stability. However, there are

differences in the response mechanisms of grassland stability to climate and biological factors. First, we found that increased biodiversity leads to increased stability of grassland ecosystems. This result was consistent with previous research that biodiversity and ecosystem stability shared a positive relationship, and biodiversity stabilized rather than enhanced grassland productivity (Pennekamp et al., 2018; Wang et al., 2019). Previous studies indicate that biodiversity stabilizes ecosystem productivity and services by increasing resistance to extreme climate events (Hossain et al., 2022; Isbell et al., 2015). We found a positive correlation between grassland ecosystem stability and biodiversity, which suggests that increased biodiversity may contribute to stability. However, compared with the experimental data, our analyses were conducted at the spatial scale of MODIS pixels, so the results obtained at such a large scale may be limited.

Second, grassland stability showed an upward trend with increasing precipitation and radiation. The main reason for this finding is that vegetation becomes less sensitive to drought as precipitation increases (Vicente-Serrano et al., 2012), and increased light during drought may maintain or enhance vegetation canopy greenness (Guo et al., 2021). In addition, we observed that grassland stability decreases along a gradient of MAP when MAP is greater than 700 mm, which may contradict the findings of some previous studies (Hoover et al., 2017; Knapp et al., 2016). One possible explanation for this is that, as MAP increases, excess water reduces grassland stability by inhibiting soil oxygen diffusion and limiting the supply of oxygen to the roots (Schuur et al., 2001). Excessive

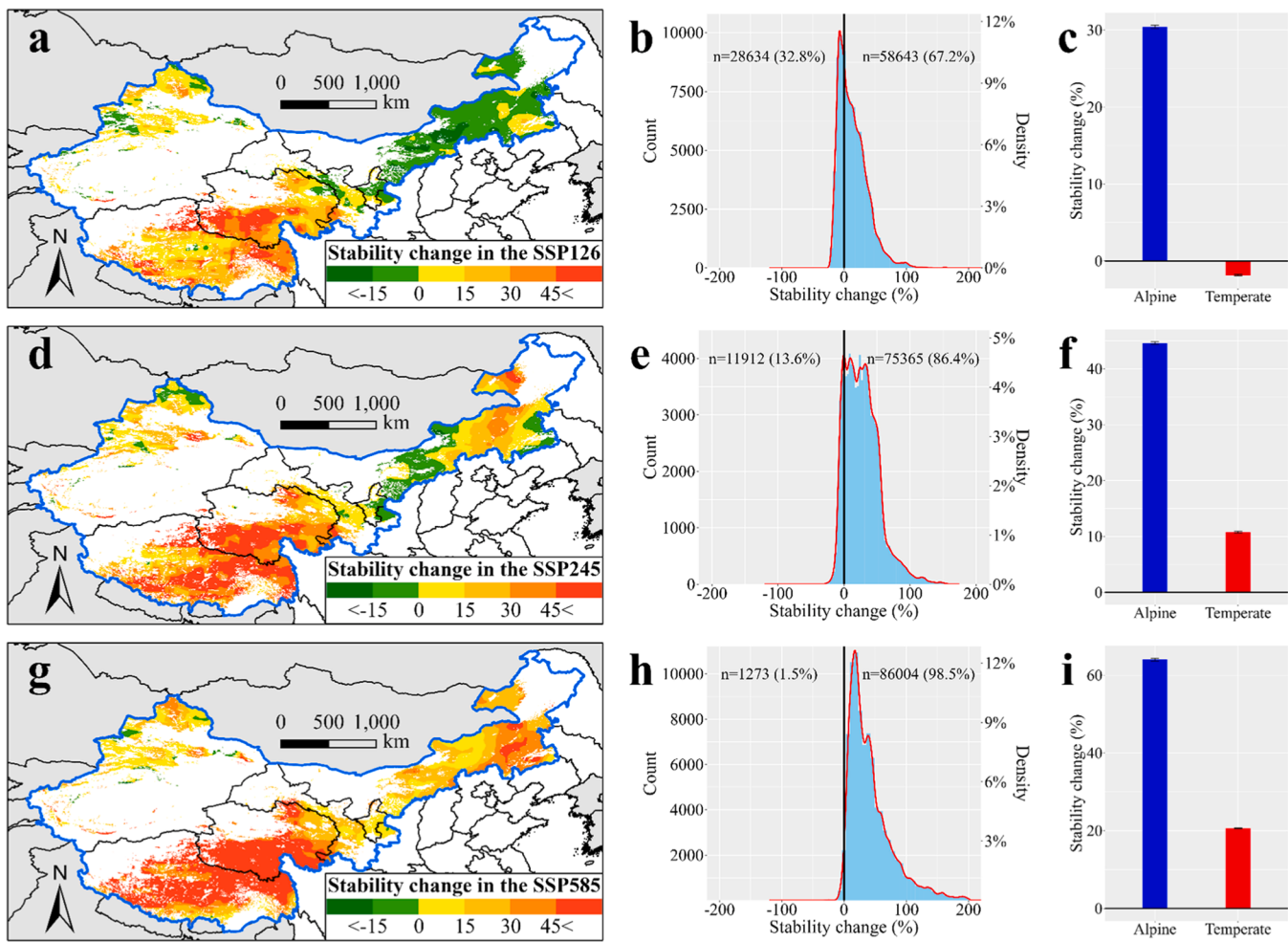


Fig. 6. Future changes (2086–2100 versus 2000–2014) in grassland stability under SSP126, SSP245, and SSP585 scenarios. (a, d, g) Spatial patterns of changes in grassland stability. (b, e, h) Density statistics of changes in grassland stability in the NCTP. (c, f, i) Mean values of changes in grassland stability within different climate zones (note: error bars represent 95 % confidence intervals).

rainfall increases soil erosion and exacerbates nutrient loss(Gao et al., 2013). Another possible explanation is that cloudy weather reduces radiation(Schuur, 2003).It should be noted that herbaceous biomes may have high drought resistance in extremely arid regions due to their specialized root/crown ratio (low aboveground biomass and high fine-root biomass), allowing them to quickly cope with drought and avoid water stress death (Vicente-Serrano et al., 2012). Thus, we observed a decrease in stability as MAP increased from 100 to 250 mm. In addition, although cloudy weather reduces radiation in temperate mountain grasslands (e.g. grasslands in the Altai and Tianshan mountains, Xinjiang), high precipitation and biodiversity still give these grasslands strong drought resistance (Fig. S7). This explains the decreasing trend in the stability as MAR increased from 3000 to 3200.

Finally, our results also revealed the non-linear response of grassland stability to temperature in the NCTP. Specifically, grassland stability increases with temperature when MAT is below 5°C, but beyond the optimal temperature, continued warming causes biochemical and stomatal limitations (Smith et al., 2020), reducing grassland stability. Related research supports our finding that warmer temperatures increase photosynthetic rates and carbon assimilation, but warming reduces grassland productivity when temperatures exceed ecosystem thresholds (Lin et al., 2010; Zhao and Running, 2010). Based on the above analyses, it can be found that the higher stability of alpine grasslands compared to temperate grasslands is due to their higher biodiversity, precipitation and radiation, and lower temperatures.

4.3. Implications and limitations

Quantifying and understanding patterns of vegetation productivity in response to drought is critical for inferring terrestrial ecosystem vulnerability and has important implications for the development of models that facilitate more accurate predictions of future terrestrial carbon sinks (Friedlingstein et al., 2014; Liu et al., 2023b; Yao et al., 2024). Our study improved the understanding of grassland stability under severe drought and contributed to the prediction of terrestrial ecosystem feedbacks to climate change by Earth system models, as well as to the identification of ecologically vulnerable areas in the NCTP under future climate change. Meanwhile, information on the stability of different grassland biomes in this study can also be a guide in adopting different ecosystem management measures to deal with future drought events.

Regional analyses of changes in grassland stability based on CMIP6 GPP data are an attempt to diagnose the ecological mechanisms underlying changes in grassland productivity in the NCTP under future climate change. Our study found that the stability of grasslands in the NCTP will increase in the future, even under the high emission scenario. However, given the negative impacts of rising temperatures on ecosystem productivity (Chen et al., 2021a; Huang et al., 2019), we are concerned that this trend may not continue. Previous studies have indicated that continued warming could exacerbate the severity and duration of future droughts (AghaKouchak et al., 2020; Miao et al., 2020). Therefore, the implementation of climate change mitigation

measures is highly desirable to avoid the risk of ecosystem collapse caused by extreme events. In addition, the results of this study suggest that an increase in biodiversity is an important factor in maintaining ecosystem stability. Therefore, to mitigate the effects of future warming on grassland productivity, appropriate management measures (e.g. fencing and sealing, reducing grazing intensity and establishing protected areas) should be taken to enhance the conservation of biodiversity in grassland ecosystems (Zhang et al., 2023a; Zhao et al., 2020; Zhu et al., 2023).

In order to accurately assess changes in ecosystem stability, it is desirable to use the same vegetation indicators for predictive analyses. Unfortunately, due to the limitation of having only GPP simulation data in CMIP6, we used GPP instead of NDVI to analyze future changes of grassland stability in the NCTP. Although NDVI and GPP have similarities in representing the growth status of vegetation, they also have differences in representing the structure and function of ecosystems (Mallick et al., 2024; Wang et al., 2020). The decoupling of structure and function may cause differences in the response of NDVI and GPP to drought. Therefore, to better interface with existing research and assess future vegetation changes, we suggest that diverse simulation data should be developed to characterize various aspects of vegetation growth.

It should be noted that our analyses of grassland productivity change under drought were largely based on a single optical vegetation index. However, leaf area index (LAI) data, solar-induced chlorophyll fluorescence (SIF) data and microwave vegetation optical depth (VOD) data have been widely used to quantify vegetation productivity (Anniwaer et al., 2024; Smith and Boers, 2023; Yao et al., 2024; Zhang et al., 2023b). Furthermore, our study does not take into account the complex response of grasslands to long-term drought at the site level, such as drought-induced grassland degradation (Li et al., 2025). Therefore, to fully understand the dynamics of grassland productivity after drought, future research will require both ground-based data and novel satellite observations to complement our findings.

5. Conclusion

We quantified the temporal stability, drought resistance and drought resilience of various grassland biomes, determined the relative importance and marginal effects of potential factors on grassland stability, and predicted future changes in grassland stability. We found significant differences in the stability among different grassland biomes, with alpine grasslands being more stable than temperate grasslands due to their greater resistance to drought. This difference in stability can be explained by the spatial heterogeneity of climatic and biological factors. Specifically, increases in biodiversity, average precipitation, and average radiation all enhance grassland stability, while lower or higher average temperature has a negative effect on grassland stability. Results based on CMIP6 indicated that the area and magnitude of the increase in grassland stability in the NCTP was significantly higher under the SSP585 scenario than under the SSP245 and SSP126 scenarios, especially in the alpine region. Given the uncertainty in current vegetation models for assessing the impacts of climate extremes such as drought, this study highlights the importance of understanding grassland stability at the process level of severe drought response. In addition, our findings further strengthen the understanding of the differential response of grassland stability to climate and biodiversity under severe drought, which is critical for assessing the future impacts of climate change on grassland growth and carbon cycling in the NCTP.

CRediT authorship contribution statement

Haile Zhao: Validation, Data curation, Writing – original draft, Software, Conceptualization, Visualization, Methodology. **Yi Zhou:** Investigation, Validation. **Xin Chen:** Validation, Investigation. **Yuan Qi:** Validation, Investigation. **Yuyang Chang:** Writing – review & editing.

Yuchao Luo: Validation. **Xingjie Yin:** Validation. **Yuling Jin:** Validation. **Zhihua Pan:** Supervision, Funding acquisition. **Pingli An:** Writing – review & editing, Conceptualization, Supervision, Funding acquisition.

Declaration of Competing Interest

The authors declare that they have no known competing financial interests or personal relationships that could have appeared to influence the work reported in this paper.

Acknowledgments

This work was supported by the National Natural Science Foundation of China [42271268] and the National Key Research and Development Program of China [2022YFD1500602–3].

Appendix A. Supporting information

Supplementary data associated with this article can be found in the online version at [doi:10.1016/j.agee.2025.109831](https://doi.org/10.1016/j.agee.2025.109831).

Data availability

Data will be made available on request.

References

- Aghakouchak, A., Chiang, F., Huning, L.S., Love, C.A., Mallakpour, I., Mazdiyasni, O., Moftakhar, H., Papalexiou, S.M., Ragni, E., Sadegh, M., 2020. Climate extremes and compound hazards in a warming world. *Annu. Rev. Earth Planet. Sci.* 48, 519–548. <https://doi.org/10.1146/annurev-earth-071719-055228>.
- Ahlström, A., Raupach, M.R., Schurges, G., Smith, B., Arneth, A., Jung, M., Reichstein, M., Canadell, J.G., Friedlingstein, P., Jain, A.K., 2015. The dominant role of semi-arid ecosystems in the trend and variability of the land CO₂ sink. *Science* 348, 895–899.
- Anniwaer, N., Li, X., Wang, K., Xu, H., Hong, S., 2024. Shifts in the trends of vegetation greenness and photosynthesis in different parts of Tibetan Plateau over the past two decades. *Agric. For. Meteorol.* 345. <https://doi.org/10.1016/j.agrformet.2023.109851>.
- Bai, Z.H., Ma, W.Q., Ma, L., Velthof, G.L., Wei, Z.B., Havlik, P., Oenema, O., Lee, M.R.F., Zhang, F.S., 2018. China's livestock transition: driving forces, impacts, and consequences. *Sci. Adv.* 4, eaar8534. <https://doi.org/10.1126/sciadv.aar8534>.
- Bengtsson, J., Bullock, J., Egoh, B., Everson, C., Everson, T., O'Connor, T., O'Farrell, P., Smith, H., Lindborg, R., 2019. Grasslands—more important for ecosystem services than you might think. *Ecosphere* 10, e02582.
- Breiman, L., 2001. Random forests. *Mach. Learn.* 45, 5–32.
- Chen, A., Huang, L., Liu, Q., Piao, S., 2021a. Optimal temperature of vegetation productivity and its linkage with climate and elevation on the Tibetan Plateau. *Glob. Change Biol.* 27, 1942–1951. <https://doi.org/10.1111/gcb.15542>.
- Chen, L., Jiang, L., Jing, X., Wang, J., Shi, Y., Chu, H., He, J.S., Bjorkman, A., 2021b. Above- and belowground biodiversity jointly drive ecosystem stability in natural alpine grasslands on the Tibetan Plateau. *Glob. Ecol. Biogeogr.* 30, 1418–1429. <https://doi.org/10.1111/geb.13307>.
- De Keersmaecker, W., Lhermitte, S., Tits, L., Honnay, O., Somers, B., Coppin, P., 2015. A model quantifying global vegetation resistance and resilience to short-term climate anomalies and their relationship with vegetation cover. *Glob. Ecol. Biogeogr.* 24, 539–548. <https://doi.org/10.1111/geb.12279>.
- Deng, Y., Wang, X., Wang, K., Ciais, P., Tang, S., Jin, L., Li, L., Piao, S., 2021. Responses of vegetation greenness and carbon cycle to extreme droughts in China. *Agric. For. Meteorol.* 298–299. <https://doi.org/10.1016/j.agrformet.2020.108307>.
- Dou, Y., Tong, X., Horion, S., Feng, L., Fensholt, R., Shao, Q., Tian, F., 2024. The success of ecological engineering projects on vegetation restoration in China strongly depends on climatic conditions. *Sci. Total Environ.* 915. <https://doi.org/10.1016/j.scitotenv.2024.170041>.
- Forzieri, G., Dakos, V., McDowell, N.G., Ramdane, A., Cescatti, A., 2022. Emerging signals of declining forest resilience under climate change. *Nature* 608, 534–539. <https://doi.org/10.1038/s41586-022-04959-9>.
- Friedlingstein, P., Meinshausen, M., Arora, V.K., Jones, C.D., Anav, A., Liddicoat, S.K., Knutti, R., 2014. Uncertainties in CMIP5 climate projections due to carbon cycle feedbacks. *J. Clim.* 27, 511–526.
- Gao, Y., Zhou, X., Wang, Q., Wang, C., Zhan, Z., Chen, L., Yan, J., Qu, R., 2013. Vegetation net primary productivity and its response to climate change during 2001–2008 in the Tibetan Plateau. *Sci. Total Environ.* 444, 356–362. <https://doi.org/10.1016/j.scitotenv.2012.12.014>.
- Guo, D., Song, X., Hu, R., Cai, S., Zhu, X., Hao, Y., 2021. Grassland type-dependent spatiotemporal characteristics of productivity in Inner Mongolia and its response to

- climate factors. *Sci. Total Environ.* 775. <https://doi.org/10.1016/j.scitotenv.2021.145644>.
- Hautier, Y., Zhang, P., Loreau, M., Wilcox, K.R., Seabloom, E.W., Borer, E.T., Byrnes, J.E., Koerner, S.E., Komatsu, K.J., Lefcheck, J.S., 2020. General destabilizing effects of eutrophication on grassland productivity at multiple spatial scales. *Nat. Commun.* 11, 5375.
- Hoover, D., Knapp, A., Smith, M., 2017. Photosynthetic responses of a dominant C 4 grass to an experimental heat wave are mediated by soil moisture. *Oecologia* 183, 303–313.
- Hossain, M.L., Li, J., Hoffmann, S., Beierkuhnlein, C., 2022. Biodiversity showed positive effects on resistance but mixed effects on resilience to climatic extremes in a long-term grassland experiment. *Sci. Total Environ.* 827. <https://doi.org/10.1016/j.scitotenv.2022.154322>.
- Huang, K., Xia, J., 2019. High ecosystem stability of evergreen broadleaf forests under severe droughts. *Glob. Change Biol.* 25, 3494–3503. <https://doi.org/10.1111/gcb.14748>.
- Huang, M., Piao, S., Ciais, P., Peñuelas, J., Wang, X., Keenan, T.F., Peng, S., Berry, J.A., Wang, K., Mao, J., Alkama, R., Cescatti, A., Cuntz, M., De Deurwaerder, H., Gao, M., He, Y., Liu, Y., Luo, Y., Myreni, R.B., Niu, S., Shi, X., Yuan, W., Verbeeck, H., Wang, T., Wu, J., Janssens, I.A., 2019. Air temperature optima of vegetation productivity across global biomes. *Nat. Ecol. Evol.* 3, 772–779. <https://doi.org/10.1038/s41559-019-0838-x>.
- Huang, W., Wang, W., Cao, M., Fu, G., Xia, J., Wang, Z., Li, J., 2021. Local climate and biodiversity affect the stability of China's grasslands in response to drought. *Sci. Total Environ.* 768. <https://doi.org/10.1016/j.scitotenv.2021.145482>.
- Isbell, F., Craven, D., Connolly, J., Loreau, M., Schmid, B., Beierkuhnlein, C., Bezemer, T.M., Bonin, C., Bruehlheide, H., de Luca, E., Ebeling, A., Griffin, J.N., Guo, Q., Hautier, Y., Hector, A., Jentsch, A., Kreyling, J., Lanta, V., Manning, P., Meyer, S.T., Mori, A.S., Naeem, S., Niklaus, P.A., Polley, H.W., Reich, P.B., Roscher, C., Seabloom, E.W., Smith, M.D., Thakur, M.P., Tilman, D., Tracy, B.F., van der Putten, W.H., van Ruijven, J., Weigelt, A., Weisser, W.W., Wilsey, B., Eisenhauer, N., 2015. Biodiversity increases the resistance of ecosystem productivity to climate extremes. *Nature* 526, 574–577. <https://doi.org/10.1038/nature15374>.
- Ivits, E., Horion, S., Fensholt, R., Cherlet, M., 2013. Drought footprint on European ecosystems between 1999 and 2010 assessed by remotely sensed vegetation phenology and productivity. *Glob. Change Biol.* 20, 581–593. <https://doi.org/10.1111/gcb.12393>.
- Ivits, E., Horion, S., Erhard, M., Fensholt, R., 2016. Assessing European ecosystem stability to drought in the vegetation growing season. *Glob. Ecol. Biogeogr.* 25, 1131–1143. <https://doi.org/10.1111/geb.12472>.
- Knapp, A.K., Ciais, P., Smith, M.D., 2016. Reconciling inconsistencies in precipitation–productivity relationships: implications for climate change. *N. Phytol.* 214, 41–47. <https://doi.org/10.1111/nph.14381>.
- Li, P., Hu, Z., Liu, Y., 2020. Shift in the trend of browning in Southwestern Tibetan Plateau in the past two decades. *Agric. For. Meteorol.* 287. <https://doi.org/10.1016/j.agrformat.2020.107950>.
- Li, S., Lu, S., Wang, X., Chen, Z., Li, B., Zhao, N., Xu, X., 2025. Drought timing and degradation status determine the grassland sensitivity to simulated drought events. *Agric. Ecosyst. Environ.* 378. <https://doi.org/10.1016/j.agee.2024.109312>.
- Lin, D., Xia, J., Wan, S., 2010. Climate warming and biomass accumulation of terrestrial plants: a meta-analysis. *N. Phytol.* 188, 187–198. <https://doi.org/10.1111/j.1469-8137.2010.03347.x>.
- Liu, D., Wang, T., Yang, T., Yan, Z., Liu, Y., Zhao, Y., Piao, S., 2019a. Deciphering impacts of climate extremes on Tibetan grasslands in the last fifteen years. *Sci. Bull.* 64, 446–454. <https://doi.org/10.1016/j.scib.2019.03.012>.
- Liu, Y., Yang, Y., Wang, Q., Du, X., Li, J., Gang, C., Zhou, W., Wang, Z., 2019b. Evaluating the responses of net primary productivity and carbon use efficiency of global grassland to climate variability along an aridity gradient. *Sci. Total Environ.* 652, 671–682. <https://doi.org/10.1016/j.scitotenv.2018.10.295>.
- Liu, Y., Men, M., Peng, Z., Chen, H.Y.H., Yang, Y., Peng, Y., 2023a. Spatially explicit estimate of nitrogen effects on soil respiration across the globe. *Glob. Change Biol.* 29, 3591–3600. <https://doi.org/10.1111/gcb.16716>.
- Liu, Z., Zhu, J., Xia, J., Huang, K., 2023b. Declining resistance of vegetation productivity to droughts across global biomes. *Agric. For. Meteorol.* 340. <https://doi.org/10.1016/j.agrformat.2023.109602>.
- Luo, W., Shi, Y., Wilkins, K., Song, L., Te, N., Chen, J., Zhang, H., Yu, Q., Wang, Z., Han, X., 2023. Plant traits modulate grassland stability during drought and post-drought periods. *Funct. Ecol.* 37, 2611–2620.
- Mallick, K., Verfaillie, J., Wang, T., Ortiz, A.A., Szutu, D., Yi, K., Kang, Y., Shortt, R., Hu, T., Sulis, M., Szantoi, Z., Boulet, G., Fisher, J.B., Baldocchi, D., 2024. Net fluxes of broadband shortwave and photosynthetically active radiation complement NDVI and near infrared reflectance of vegetation to explain gross photosynthesis variability across ecosystems and climate. *Remote Sens. Environ.* 307. <https://doi.org/10.1016/j.rse.2024.114123>.
- Miao, L., Li, S., Zhang, F., Chen, T., Shan, Y., Zhang, Y., 2020. Future drought in the dry lands of Asia under the 1.5 and 2.0°C warming scenarios. *Earth'S. Future* 8, e2019EF001337.
- Moen, J., Ellis, E.C., Antill, E.C., Kreft, H., 2012. All Is Not Loss: Plant Biodiversity in the Anthropocene. *PLoS ONE* 7. <https://doi.org/10.1371/journal.pone.0030535>.
- Montoya, D., Haegeman, B., Gaba, S., de Mazancourt, C., Bretagnolle, V., Loreau, M., 2019. Trade-offs in the provisioning and stability of ecosystem services in agroecosystems. *Ecol. Appl.* 29. <https://doi.org/10.1002/earp.1853>.
- Muraina, T.O., Xu, C., Yu, Q., Yang, Y., Jing, M., Jia, X., Jaman, M.S., Dam, Q., Knapp, A.K., Collins, S.L., 2021. Species asynchrony stabilizes productivity under extreme drought across Northern China grasslands. *J. Ecol.* 109, 1665–1675.
- Pennekamp, F., Pontarp, M., Tabi, A., Altermatt, F., Alther, R., Choffat, Y., Frohofer, E.A., Ganeshanandamoorthy, P., Garnier, A., Griffiths, J.I., 2018. Biodiversity increases and decreases ecosystem stability. *Nature* 563, 109–112.
- Piao, S., Wang, X., Ciais, P., Zhu, B., Wang, T.A.O., Liu, J.I.E., 2011. Changes in satellite-derived vegetation growth trend in temperate and boreal Eurasia from 1982 to 2006. *Glob. Change Biol.* 17, 3228–3239. <https://doi.org/10.1111/j.1365-2486.2011.02419.x>.
- Piao, S., Zhang, X., Chen, A., Liu, Q., Lian, X., Wang, X., Peng, S., Wu, X., 2019. The impacts of climate extremes on the terrestrial carbon cycle: A review. *Sci. China Earth Sci.* 62, 1551–1563. <https://doi.org/10.1007/s11430-018-9363-5>.
- Piao, S., Wang, X., Park, T., Chen, C., Lian, X., He, Y., Bjerke, J.W., Chen, A., Ciais, P., Tømmervik, H., 2020. Characteristics, drivers and feedbacks of global greening. *Nat. Rev. Earth Environ.* 1, 14–27.
- Ponce-Campos, G.E., Moran, M.S., Huete, A., Zhang, Y., Bresloff, C., Huxman, T.E., Eamus, D., Bosch, D.D., Buda, A.R., Gunter, S.A., Scalley, T.H., Kitchen, S.G., McClaran, M.P., McNab, W.H., Montoya, D.S., Morgan, J.A., Peters, D.P.C., Sadler, E.J., Seyfried, M.S., Starks, P.J., 2013. Ecosystem resilience despite large-scale altered hydroclimatic conditions. *Nature* 494, 349–352. <https://doi.org/10.1038/nature11836>.
- Poulter, B., Frank, D., Ciais, P., Myreni, R.B., Andela, N., Bi, J., Broquet, G., Canadell, J.G., Chevallier, F., Liu, Y.Y., Running, S.W., Sitch, S., van der Werf, G.R., 2014. Contribution of semi-arid ecosystems to interannual variability of the global carbon cycle. *Nature* 509, 600–603. <https://doi.org/10.1038/nature13376>.
- Schuur, E.A.G., 2003. Productivity and Global Climate Revisited: The Sensitivity of Tropical Forest Growth To Precipitation. *Ecology* 84, 1165–1170. [https://doi.org/10.1890/0012-9658\(2003\)084\[1165:Pgct\]2.0.Co;2](https://doi.org/10.1890/0012-9658(2003)084[1165:Pgct]2.0.Co;2).
- Schuur, E.A.G., Chadwick, O.A., Matson, P.A., 2001. Carbon Cycling and Soil Carbon Storage in Mesic To Wet Hawaiian Montane Forests. *Ecology* 82, 3182–3196. [https://doi.org/10.1890/0012-9658\(2001\)082\[3182:Ccas\]2.0.Co;2](https://doi.org/10.1890/0012-9658(2001)082[3182:Ccas]2.0.Co;2).
- Schwalm, C.R., Anderegg, W.R.L., Michalak, A.M., Fisher, J.B., Biondi, F., Koch, G., Litvak, M., Ogle, K., Shaw, J.D., Wolf, A., Huntzinger, D.N., Schaefer, K., Cook, R., Wei, Y., Fang, Y., Hayes, D., Huang, M., Jain, A., Tian, H., 2017. Global patterns of drought recovery. *Nature* 548, 202–205. <https://doi.org/10.1038/nature23021>.
- Seddon, A.W.R., Macias-Fauria, M., Long, P.R., Benz, D., Willis, K.J., 2016. Sensitivity of global terrestrial ecosystems to climate variability. *Nature* 531, 229–232. <https://doi.org/10.1038/nature16986>.
- Sippel, S., Reichstein, M., Ma, X., Mahecha, M.D., Lange, H., Flach, M., Frank, D., 2018. Drought, heat, and the carbon cycle: a review. *Curr. Clim. Change Rep.* 4, 266–286.
- Slette, I.J., Post, A.K., Awad, M., Even, T., Punzalan, A., Williams, S., Smith, M.D., Knapp, A.K., 2019. How ecologists define drought, and why we should do better. *Glob. Change Biol.* 25, 3193–3200. <https://doi.org/10.1111/gcb.14747>.
- Smith, M.D., Wilkins, K.D., Holdrege, M.C., Wilfahrt, P., Collins, S.L., Knapp, A.K., Sala, O.E., Dukes, J.S., Phillips, R.P., Yahdjian, L., 2024. Extreme drought impacts have been underestimated in grasslands and shrublands globally. *Proc. Natl. Acad. Sci.* 121, e2309881120.
- Smith, M.N., Taylor, T.C., van Haren, J., Rosolem, R., Restrepo-Coupe, N., Adams, J., Wu, J., de Oliveira, R.C., da Silva, R., de Araujo, A.C., de Camargo, P.B., Huxman, T.E., Saleska, S.R., 2020. Empirical evidence for resilience of tropical forest photosynthesis in a warmer world. *Nat. Plants* 6, 1225–1230. <https://doi.org/10.1038/s41477-020-00780-2>.
- Smith, T., Boers, N., 2023. Global vegetation resilience linked to water availability and variability. *Nat. Commun.* 14. <https://doi.org/10.1038/s41467-023-36207-7>.
- Van Ruijven, J., Berendse, F., 2010. Diversity enhances community recovery, but not resistance, after drought. *J. Ecol.* 98, 81–86.
- Vicente-Serrano, S.M., Beguería, S., López-Moreno, J.I., 2010. A multiscalar drought index sensitive to global warming: the standardized precipitation evapotranspiration index. *J. Clim.* 23, 1696–1718.
- Vicente-Serrano, S.M., Gouveia, C., Camarero, J.J., Beguería, S., Trigo, R., López-Moreno, J.I., Azorín-Molina, C., Pasho, E., Lorenzo-Lacruz, J., Revuelto, J., Morán-Tejeda, E., Sanchez-Lorenzo, A., 2012. Response of vegetation to drought time-scales across global land biomes. *Proc. Natl. Acad. Sci.* 110, 52–57. <https://doi.org/10.1073/pnas.1207068110>.
- Wang, R., Gamon, J.A., Emmerton, C.A., Springer, K.R., Yu, R., Hmimina, G., 2020. Detecting intra- and inter-annual variability in gross primary productivity of a North American grassland using MODIS MAIAC data. *Agric. For. Meteorol.* 281. <https://doi.org/10.1016/j.agrformat.2019.107859>.
- Wang, Y., Cadotte, M.W., Chen, Y., Fraser, L.H., Zhang, Y., Huang, F., Luo, S., Shi, N., Loreau, M., 2019. Global evidence of positive biodiversity effects on spatial ecosystem stability in natural grasslands. *Nat. Commun.* 10. <https://doi.org/10.1038/s41467-019-11191-z>.
- Xia, H., Yuan, S., Prishchepov, A.V., 2023. Spatial-temporal heterogeneity of ecosystem service interactions and their social-ecological drivers: Implications for spatial planning and management. *Resour. Conserv. Recycl.* 189. <https://doi.org/10.1016/j.resconrec.2022.106767>.
- Yang, J., Huang, X., 2021. The 30 m annual land cover dataset and its dynamics in China from 1990 to 2019. *Earth Syst. Sci. Data* 13, 3907–3925. <https://doi.org/10.5194/essd-13-3907-2021>.
- Yang, Y., Yuan, X., An, J., Su, Q., Chen, B., 2024. Drivers of ecosystem services and their trade-offs and synergies in different land use policy zones of Shaanxi Province, China. *J. Clean. Prod.* 452. <https://doi.org/10.1016/j.jclepro.2024.142077>.
- Yao, Y., Liu, Y., Fu, F., Song, J., Wang, Y., Han, Y., Wu, T., Fu, B., 2024. Declined terrestrial ecosystem resilience. *Glob. Change Biol.* 30. <https://doi.org/10.1111/gcb.17291>.
- Zhang, C., Long, D., Liu, T., Slater, L.J., Wang, G., Zuo, D., Duan, L., Cui, Y., Cui, Y., 2023a. Grassland greening and water resource availability may coexist in a warming

- climate in Northern China and the Tibetan Plateau. *Earth'S. Future* 11. <https://doi.org/10.1029/2023ef004037>.
- Zhang, X., Sun, S., Yong, S., Zhou, Z., Wang, R., 2007. Vegetation map of the People's Republic of China (1: 1000000). Geol. Publ. House.
- Zhang, Y., Song, C., Band, L.E., Sun, G., Li, J., 2017. Reanalysis of global terrestrial vegetation trends from MODIS products: Browning or greening? *Remote Sens. Environ.* 191, 145–155. <https://doi.org/10.1016/j.rse.2016.12.018>.
- Zhang, Y., Liu, X., Jiao, W., Wu, X., Zeng, X., Zhao, L., Wang, L., Guo, J., Xing, X., Hong, Y., 2023b. Spatial Heterogeneity of Vegetation Resilience Changes to Different Drought Types. *Earth'S. Future* 11. <https://doi.org/10.1029/2022ef003108>.
- Zhang, Y., Hong, S., Liu, D., Piao, S., 2023a. Susceptibility of vegetation low-growth to climate extremes on Tibetan Plateau. *Agric. For. Meteorol.* 331. <https://doi.org/10.1016/j.agrformet.2023.109323>.
- Zhao, M., Running, S.W., 2010. Drought-induced reduction in global terrestrial net primary production from 2000 through 2009. *Science* 329, 940–943. <https://doi.org/10.1126/science.1192666>.
- Zhao, W., Hu, Z., Guo, Q., Wu, G., Chen, R., Li, S., 2020. Contributions of climatic factors to interannual variability of the vegetation index in Northern China Grasslands. *J. Clim.* 33, 175–183.
- Zhou, L., Tian, Y., Myneni, R.B., Ciais, P., Saatchi, S., Liu, Y.Y., Piao, S., Chen, H., Vermote, E.F., Song, C., 2014. Widespread decline of Congo rainforest greenness in the past decade. *Nature* 509, 86–90.
- Zhu, Q., Chen, H., Peng, C., Liu, J., Piao, S., He, J.-S., Wang, S., Zhao, X., Zhang, J., Fang, X., Jin, J., Yang, Q.-E., Ren, L., Wang, Y., 2023. An early warning signal for grassland degradation on the Qinghai-Tibetan Plateau. *Nat. Commun.* 14. <https://doi.org/10.1038/s41467-023-42099-4>.
- Zscheischler, J., Mahecha, M.D., von Buttlar, J., Harmeling, S., Jung, M., Rammig, A., Randerson, J.T., Schölkopf, B., Seneviratne, S.I., Tomelleri, E., Zaehle, S., Reichstein, M., 2014. A few extreme events dominate global interannual variability in gross primary production. *Environ. Res. Lett.* 9. <https://doi.org/10.1088/1748-9326/9/3/035001>.